Softening of the Euler buckling criterion under discretization of compliance

D.J. Carter
School of Physics and Astronomy, Queen Mary University of London, London E1 4NS

D.J. Dunstan*
School of Physics and Astronomy, Queen Mary University of London, London E1 4NS, United Kingdom

W. Just and O.F. Bandtlow
School of Mathematical Sciences, Queen Mary University of London, London E1 4NS, United Kingdom

A. San-Miguel
Université de Lyon, F-69000 Lyon, France and Institut Lumière Matière, CNRS, UMR 5306, Université Lyon 1, F-69622 Villeurbanne, France

(Dated: October 21, 2021)

Euler solved the problem of the collapse of tall thin columns under unexpectedly small loads in 1744. The analogous problem of the collapse of circular elastic rings or tubes under external pressure was mathematically intractable and only fully solved recently. In the context of carbon nanotubes, an additional phenomenon was found experimentally and in atomistic simulations but not explained: the collapse pressure of smaller diameter tubes deviates below the continuum mechanics solution [Torres-Dias *et al.*, Carbon **123**, 145 (2017)]. Here, this deviation is shown to occur in discretized straight columns and it is fully explained in terms of the phonon dispersion curve. This reveals an unexpected link between the static mechanical properties of discrete systems and their dynamics described through dispersion curves.

The tendency of tall thin columns to collapse under unexpectedly small loads was already known to the ancient Greeks - it is suggested that their use of entasis (Fig.1a) was to strengthen columns [1], and the Romans based their structures on short fat columns, as in the Pont du Gard (Fig.1b). The phenomenon was explained by Euler in a classic work [2]; his explanation is now usually expressed in terms of the elastic energy required for a lateral deflection of the column compared with the work done by the advance of the load for the same deflection.

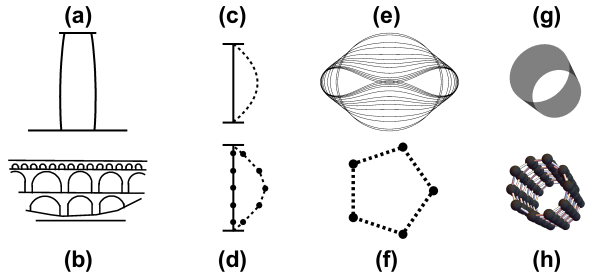

FIG. 1. (a) Entasis in Greek columns (exaggerated). (b) Schematic of the Pont du Gard. (c) A continuous pillar, buckling (dashed). (d) A discretized pillar, buckling (dashed). (e) The collapse of a continuous elastic ring. (f) A discretized elastic ring (a polygon). (g) A continuous tube. (h) An example of a discretized tube (a nanotube) [a]

[a] http://demonstrations.wolfram.com/NanotubeBuilder/

The collapse of circular tubes under external pressure follows the same simple physics, but is mathematically intractable. Although it was of great importance in early steam engine boilers, and later in oil wells, engineers had to rely on empirical testing [3, 4], as only partial theoretical solutions were available [5, 6] . The full solution for the post-buckling behaviour of a continuous thin elastic ring was given only in 2011 [7, 8]. However, here we are concerned only with the pressure at the onset of collapse. If the continuum solution is normalized against the bending stiffness of the tube wall, D, and the radius, r, of the tube, this, $P_{\rm C} = 3D/r^3$, can be expressed as $P_{\rm C}^{\rm N} = P_{\rm C} r^3/D = 3$ [5, 6, 9].

In a recent study of the collapse pressure of single-wall carbon nanotubes [10], a surprising result was reported. Small-diameter tubes collapse at pressures lower than the continuum solution. Experimental measurements and simulations (molecular dynamics and density-functional modelling) were in agreement in finding $P_{\rm C}^{\rm N} = 3(1-\beta^2/d^2)$ (d is diameter), with a value of β about 0.4nm (this is therefore the diameter of the smallest stable free-standing nanotubes). Both the analytic form of this expression and the value of β were wholly unexplained [10, 11].

Nanotubes are not continuous elastic rings, as they have radii of only a few atoms. To find the collapse pressure of discretized elastic rings, Sun *et al.* [12] modelled them as polygons of area A with rigid sides joined by angular springs at the vertices (spring constant c), under an external pressure, P. The total energy is written as a function of the angles φ of the hinges, $\sum 1/2\, c\, \varphi^2 + PA$, and minimized. Results were similar, but still unexplained.

Here we set out to find an explanation by investigat-

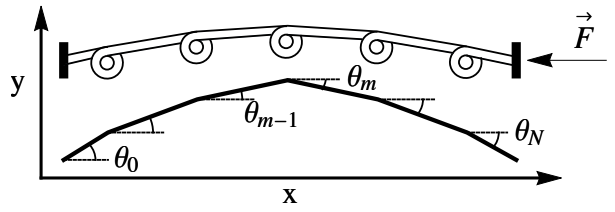

FIG. 2. A pillar along the x-axis is discretized to have compliance only at N angular hinges of stiffness c. The lower part of the graph shows a chain of rigid rods numbered $\mu = 0$ to N at angles θ_μ. Buckling causes y-axis displacements of the hinges y_μ ($\mu = 1$ to N).

ing the simpler problem of Euler's column, but atomistic or discretized. Three methods, numerical, analytic and dynamical, reveal the same phenomenon, with results fitting an expression for the normalised critical force $F_{\rm C}^{\rm N}$ of the same form (but different constants) as for $P_{\rm C}^{\rm N}$ above. But the results do not elucidate why it occurs nor explain the value of the constant β^2. A fourth method, recasting the problem in terms of waves on an infinitely long column, does provide a theoretical explanation in terms of the dispersion curve $\omega(k)$. Moreover, it shows that the empirical expression for $F_{\rm C}^{\rm N}$ is not exact, and it predicts the value of β^2 correctly. This approach reveals a link between the static mechanical properties of discrete systems and phonon dispersion curves.

In continuum mechanics, a column of length L with unconstrained ends and a bending stiffness, D (defined by $E = {}^1\!/_2 DR^{-2}$ where R is the radius of curvature and E is the stored elastic energy per unit length) has a buckling force of $F_{\rm C} = \pi^2 D/L^2$. This force is to be applied along the column axis. The normalized collapse force, $F_{\rm C}^{\rm N} = F_{\rm C}L^2/D$, is thus $\pi^2 \approx 9.870$. In what follows we work only with the normalised problem ($L = 1, D = 1$), except where it is useful to keep these quantities explicit. We divide the column into N equal lengths ($a_0 = 1/N$) and then move all the compliance $S = a_0/D = 1/N$ in each length to the centre of that length. That gives $N+1$ rigid links or rods, at angles θ to the column axis, joined by the compliant hinges, stiffness $c = N$, bent through angles φ (note that $\varphi_\mu = \theta_\mu - \theta_{\mu-1}$). The two end rods are half the length of the others. Concentrating the compliance in this way does indeed give a reduction in the normalized collapse force for small N. One might think, by considering the case of $N = 1$, that the compliance has been moved from where, in a continuous column, much of it is wasted (regions of smaller curvature), to the point of maximum curvature. That explanation is, however, valid only for $N = 1$. For larger N, a simple calculation shows that as much compliance has been moved to where it is less useful as to where it is more useful (see Supplemental Material (SM)§I) [13].

First, we use the numerical method of Sun *et al.* [12]. For each load F the energy is minimized with respect to the angles of the hinges, and as F is increased, the collapse force is detected by the first departure of these angles from zero (see SM §II.1)[13]. The calculations confirm that the collapse force is reduced below π^2 at small N for the discretized columns, as for the polygons. However, the calculations give no hint of the reason for this behaviour. The numerical results, plotted in Fig.3, do not contain any information on how they arise. Clearly, less elastic energy is stored in the discrete springs for a given advance of the force - but why? These numerical values of F_C^N for discrete N cannot be reverse-engineered for a general form for all N.

It is not difficult to find analytic expressions for the collapse force for each N. This is done by relating the moment on a hinge to its angle (SM §II.2) [13]. In this way, for $N = 1$, the normalized collapse force is found to be 4, for $N = 5$ it is $\frac{25}{2}(3-\sqrt{5}) \approx 9.549$ and for $N = 6$ it is $36(2-\sqrt{3}) \approx 9.646$, in agreement with the numerical calculations. However, these exact expressions for the analytic solutions for each N again do not reveal the reason for this behaviour, nor lead to a general expression in N.

An alternative, dynamical approach is to calculate the lateral oscillation frequency of the column as a function of the longitudinal compression or tension. The equation of motion for the $\mu^{\rm th}$ hinge in a chain of point-mass hinges is readily written down, if we attribute an arbitrary density $\rho = 1$ to the continuous column and then concentrate the mass $m = \rho a_0$ as well as the compliance at the hinges. The force on the $\mu^{\rm th}$ hinge comes from its own torque, exerting a force on the two adjacent hinges, plus the torques of these two hinges exerting forces on itself, and from the compression (or tension) and its own angle. That is, it depends on three term: $\varphi_{\mu\pm1}$ and φ_μ. The shorter end rods and the end hinges have to be treated differently. See SM §II.3 [13].

The equations of motion for the N hinges can be written down in matrix form, and then diagonalizing the matrix gives the frequencies as the eigenvalues. The eigenvectors describe the modes of oscillation; we are interested only in the lowest mode in which all hinges move in the same direction. The collapse force is found by setting the eigenvalue of this mode to zero and solving for the force (SM §II.3) [13]. These results of course agree with the previous calculations, but again give no hint as to the physical reason for the phenomenon.

The explanation is found by developing the dynamical method by removing the restriction of the finite column length, L, and the restriction that N is an integer (N now becomes the number of hinges per unit length). We let μ take all values from $-\infty$ to ∞, and there are now no end segments to be treated differently. Instead of diagonalizing the resulting infinite matrix, we apply Bloch's theorem [14]. This is done in SM §II.4 [13], and it gives the normalised phonon dispersion curve $\omega(k)$ for all (con-

tinuous) $N \in \mathbf{R}$,

$$\omega(k) = 2N^2 \sin\left(\frac{k}{2N}\right)\sqrt{2 - \frac{F}{N^2} - 2\cos\frac{k}{N}} \qquad (1)$$

This dispersion relation is interesting because it has solutions for negative tension, i.e. compression F, and it gives the collapse force at zero frequency. Equating the term in the square root to zero gives

$$F_{\rm C}^{\rm N} = 2N^2\left(1 - \cos\frac{k}{N}\right) \qquad (2)$$

As the problem is set up, these solutions are unphysical, because an infinite or indefinitely long system will collapse even under an indefinitely small compression. However, we can extract interesting special cases which are physically realisable. First, we are not interested in running waves, but in standing waves, because we can set the wavelength λ of a standing wave. Imposing the constraint $y = 0$ every half-wavelength along the chain determines the positions of the nodes of a standing wave of wavelength λ, without affecting its frequency. This also prevents buckling of the chain under smaller compression at wavelengths longer than λ. We can do this for the special cases where the half-wavelength $\lambda/2 = \pi/k$ is an integer multiple of the length a_0, i.e. $k = \pi/(Na_0)$, and even more specifically we can then set the nodes halfway between two hinges. With normalisation, this sets $\lambda/2$ to unity, k to π, and restricts N to integer values. In this way the section between two adjacent nodes replicates the model of Fig.2. The compressive force at which Eq.(2) gives zero frequency is, precisely, the Euler buckling force for the finite, half-wavelength system, the solutions for which can be picked out from Eq.(2) at integer N.

Eq.(2) is plotted in Fig.3 as the solid curve, which passes exactly through the solid circle datapoints from the previous solutions for integer N. In particular, the data point for $N = 1$ is accurately fitted. This fourth method does provide the explanation of the softening of the Euler buckling force in the discretised column. It is equivalent to the general sublinearity of the dispersion relation of phonon modes, $\omega(k)$, which softens the phonon frequency as the wavevector approaches the edge of the first Brillouin zone—it is the same physics.

Returning to Eq.(2) and keeping N as a real number, the expression for $F_{\rm C}^{\rm N}$ can be expanded as a polynomial in N^{-2}. Dropping the higher-order terms, that gives

$$F_{\rm C}^{\rm N}(N) = k^2\left(1 - \frac{k^2}{12N^2}\right) = \pi^2\left(1 - \frac{\beta^2}{N^2}\right) \qquad (3)$$

with $k = \pi$, giving $\beta^2 = \pi^2/12$.

Eq.(3) is plotted in Fig.3 to show that the truncation of the polynomial expansion of Eq.(2) at N^{-2} introduces only a small error for the column collapse forces for large N. The true value of β^2 is 0.8224... and the slope of the linear fit to the datapoints shown ($N - 2, 3, 4, 6, \infty$) is substantially less, at 0.7453. However, the fit residuals are tiny, the largest being 0.02. It would be natural to fit Eq.(3) to these data, to suppose the $N = 1$ datum to be anomalous, (perhaps by the simple argument of SM section 1), and to seek physical explanations for Eq.(3), for the value $\beta^2 = 0.745$, for the tiny residuals, and for the apparently anomalous $N = 1$ datapoint. Similarly, for the polygon data plotted in Fig.3, to seek physical explanations why Eq.(3) fits so well, why here $\beta^2 = 0.53$, and perhaps why the $N = 6$ point has a relatively large residual.

The experimental data of Torres-Dias *et al.* [10] is also shown in Fig.3 (their simulation data is omitted for clarity but it behaves very similarly). For these data the y-axis is numerically in units of normalised collapse

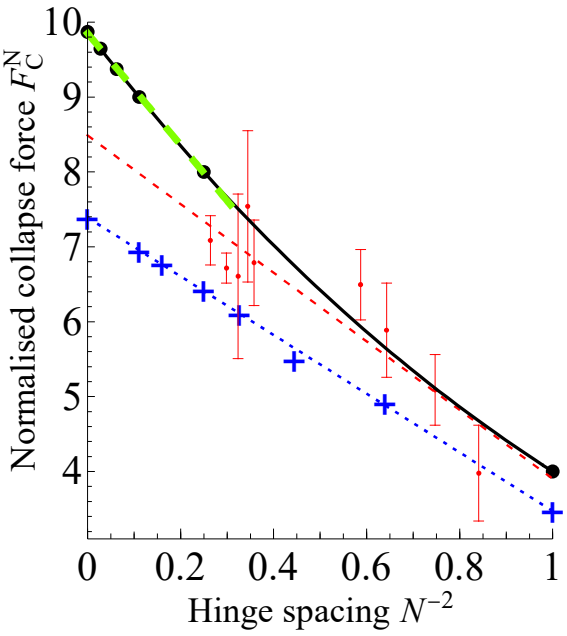

FIG. 3. The normalized collapse force $F_{\rm C}^{\rm N}$ of Eq. (2) is plotted against N^{-2} where N is the number of hinges per half-wavelength of a buckling mode of an infinite chain with $k = \pi$ (solid black line), or, equivalently, the number of hinges in a column of unity length. Results from calculations for integer N are plotted (solid circles), for $N = 1 - 4, 6, \infty$. The green dashed line is the least-squares fit of Eq.(3) to these data excluding $N = 1$.

The blue crosses are the numerical data for the collapse of m-gons [12], plotted for $m = 4 - 8, 10, 12, \infty$. This data is rescaled by converting pressure to circumferential force, and using $m = 4N$. The blue dotted line is the least-squares fit to these data. The experimental data for nanotubes [10] are shown by red datapoints with error bars and fitted by the red dashed line, scaled to these axes as described in the text.

pressure, GPa nm^3, and the x-axis is numerically in units of $^1/_2d^2$ with d in nm, in order to accommodate these data on the same graph and show the similar behaviour. It is by chance, and of no significance, that the red dashed line fitted to the data converges closely onto the pillar results at $x = 1$. It is also by chance, not design, that the polygon fit and the nanotube fit have very similar x-axis intercepts, of 1.87 and 1.85 respectively; what this may signify is not known. However, the similar behaviour of the experimental data explains why Torres-Dias *et al.* [10] fitted the data with Eq.(3).

It is interesting that the three direct attacks on the problem as stated fail because they only give discrete solutions for integer N. It is by discarding this constraint in the fourth method, discarding the boundary conditions, that a solution for all $N \in \mathbf{R}$ is found, which gives the true functional form. The results for $N \in \mathbf{Z}$ can be picked out from it, but are explained by the more general solution. The reverse process, of finding the general solution for $N \in \mathbf{R}$ from the discrete solutions for $N \in \mathbf{Z}$, and hence the explanation, is not obviously possible.

An early approximation for the problem of the elastic ring was to equate the tangential force at collapse to the collapse force of a column of length one quarter of the circumference. Levy [5] appreciated that this is not exact, and in fact gives a normalized collapse pressure of 4 instead of the correct value of 3. This is why the numerical calculations for the collapse pressure of polygons [12] rescaled for the same wavelength of collapse as the column, and converted from pressure to circumferential force, have the prefactor $\frac{3}{4}\pi^2$ instead of π^2 as seen in Fig.3.

We set out to explain the reduction of the collapse pressure of atomistic rings or tubes such as carbon nanotubes at small diameters. We have shown that is the consequence of small numbers of discrete bodies in an Eulerian buckling wavelength. There remains two practical omissions for future work. The first is the extension of these calculations to discretized circular rings (polygons), where we do not expect the value of β^2 to be the same as for straight columns. The second is the scaling factors between the value of β^2 for simple polygonal rings and for carbon nanotubes (Fig.3 would appear to imply that the smallest nanotube in the experimental dataset, chirality (8, 3), has between four and five hinges around its circumference). This can be investigated by standard techniques, such as the study of structures intermediate in complexity between carbon nanotubes and linear discretized columns. More fundamentally, attributing the reduction of the collapse pressure to the properties of the phonon dispersion curve might be considered to be a complete explanation of the phenomenon under study, or it might be considered to beg the question, why does the phonon dispersion curve behave in this way? We are not aware of a good answer to this question. Very generally, the phase velocity of a wave, given by the square root of stiffness over inertia (mass density), decreases as the wavelength is reduced toward the lattice constant. Viewed macroscopically, should this be interpreted as a decrease in the effective stiffness? That would be completely consistent with the comment above that discretisation results in less stored energy for a given advance of the force. Whatever that explanation may be, it would then fully explain why the Euler buckling force decreases when a_0 of a discretized pillar approaches L.

This is not only an issue at the atomic scale. Macroscopic structures that might ideally be continuous linear or curved structures are sometimes discretised in macroscopic sections. An example is the medical stent, intended to hold arteries open, and therefore subject to external loading. Stents would ideally be cylindrical, but they are designed to be inserted in a collapsed form and expanded once in place. So stents are commonly polygonal in section, and depending on how the compliance is distributed, may be weakened against collapse by discretisation of the compliance.

Of course, $\omega(k)$ relationships are often derived without any reference to scale – indeed, we follow a standard derivation here for Eq.(1) [15]. And it is commonplace that phonon softening under pressure is related to structural phase transitions. Nevertheless, in condensed matter physics, there is a strong tendency to consider that phenomena arising on the atomic scale are properties of the very small, and fully explained by a quantum-mechanical derivation invoking e.g. Bloch's theorem, without considering if the same phenomena would arise at the macroscopic scale. Yet here the reduction in collapse pressure is the same if a_0 is 1m or 3ÃĚ, for the same N. The static properties, in particular the structural failure, of structures at all scales are here linked to the softening of acoustic phonon modes as wavelengths approach the atomic scale.

DJD is grateful to the University of Lyons 1 (Labex iMust) for support for the initiation of this work.

* d.dunstan@qmul.ac.uk

[1] P. Thompson, G. Papadopoulou, and E. Vassiliou, The origins of entasis: Illusion, aesthetics or engineering?, Spatial Vision **20**, 531 (2007).
[2] W. A. Oldfather, C. A. Ellis, and D. M. Brown, Leonhard Euler's elastic curves, Isis **20**, 72 (1933).
[3] M. L. E. Fletcher, On the Lancashire boiler, its construction, equipment, and setting, Proceedings of the Institution of Mechanical Engineers **27**, 59 (1876).
[4] S. J. Thompson, Boilers – Past and Present, Proceedings of the Institution of Mechanical Engineers **148**, 132 (1942).
[5] M. Lévy, Mémoire sur un nouveau cas intégrable du probléme de l'élastique et l'une des ses applications, Journal de Mathématiques Pures et Appliquées **10**, 5 (1884).
[6] G. L. Carrier, On the buckling of elastic rings, J. Math.

and Phys. **26**, 94 (1947).
[7] P. Djondjorov, V. Vassilev, and I. Mladenov, Analytic description and explicit parametrisation of the equilibrium shapes of elastic rings and tubes under uniform hydrostatic pressure, International Journal of Mechanical Sciences **53**, 355 (2011).
[8] V. M. Vassilev, P. A. Djondjorov, and I. M. Mladenov, Comment on shape transition of unstrained flattest single-walled carbon nanotubes under pressure [J. Appl. Phys. 115, 044512 (2014)], Journal of Applied Physics **117**, 196101 (2015).
[9] J. Courbon, Flambement des poutres circulaires, Annales de l'Institut Technique du Batiment et des Travaux Publics, Série Theories et Methodes de Calcul **69**, 804 (1965).
[10] A. C. Torres-Dias, T. F. Cerqueira, W. Cui, M. A. Marques, S. Botti, D. Machon, M. A. Hartmann, Y. Sun, D. J. Dunstan, and A. San-Miguel, From mesoscale to nanoscale mechanics in single-wall carbon nanotubes, Carbon **123**, 145 (2017).
[11] Y. Magnin, F. Rondepierre, W. Cui, D. J. Dunstan, and A. San-Miguel, Carbon nanotubes collapse phase diagram with arbitrary number of walls. Collapse modes and macroscopic analog, Carbon **178**, 552 (2021).
[12] Y. Sun, D. Dunstan, M. Hartmann, and D. Holec, Nanomechanics of Carbon Nanotubes, PAMM **13**, 7 (2013).
[13] (2021), see Supplemental Material at [URL will be inserted by publisher] for details of the mathematics.
[14] N. Ashcroft and N. Mermin, *Solid State Physics* (Saunders College, Philadelphia, 1976).
[15] A. Fetter and J. Walecka, *Theoretical Mechanics of Particles and Continua*, Dover Books on Physics (Dover Publications, 2012).